Measurement of the proton-air inelastic cross section with ARGO-YBJ

A. Surdo[1] for the ARGO-YBJ Collaboration

***Abstract*— ARGO-YBJ, located in the Cosmic Ray Observatory of Yangbajing (Tibet, P.R.China) at $4300\ m\ a.s.l.$, is a full-coverage Extensive Air Shower array consisting of a layer of Resistive Plate Chambers (RPC) of about $6000\ m^2$. One of the main aims of the experiment is the cosmic ray physics in the $10^{12} - 10^{16}\ eV$ primary energy range, where the transition from direct to indirect measurements occurs. In this work the measurement of the interaction cross section between primary protons and air nuclei is reported. The analysis is based on the different flux attenuation for different atmospheric depths (i.e. zenith angles), by exploiting the detector capabilities in selecting the shower development stage by means of the size, hit density and both time and lateral profile measurements. The systematic errors introduced by fluctuations in shower development and heavier primaries have been taken into account. The results give useful insights on the p-air interactions at energies where models start to give significantly different expectations and allow to infer the p-p total cross section in an energy region ($\sqrt{s} = 50\ GeV - 1\ TeV$) still scarcely explored.**

I. INTRODUCTION

The cross sections involved in hadronic interactions are of great interest in particle physics. In the last decades, high-energy proton-antiproton ($p\overline{p}$) colliders have extended the measurements up to center-of-mass energy $\sqrt{s} = 1.8\ TeV$ and the CERN Large Hadron Collider (LHC) will study proton-proton (p-p) collisions up to $\sqrt{s} = 14\ TeV$. Anyway, at energies exceeding $\sqrt{s} \sim 70\ GeV$, the knowledge on the increase of the hadronic cross section as a function of energy is limited by experimental errors and/or lack of data. For instance, the values of the total $p\overline{p}$ cross section as measured at the Tevatron ($\sqrt{s} = 1.8\ TeV$) disagree by about 10% between different experiments [1], [2], [3].

Cosmic ray data provide an unique opportunity to study proton interactions in an energy range which covers not only the energy of the LHC, but extends well beyond it, since the natural beam of cosmic ray particles spans up to extreme energies. The measurement of the distribution of X_0, the first proton-air (p-air) interaction point, would give the absorption of the primary proton flux while penetrating the atmosphere, thus allowing, in principle, to measure in a straight-forward way the mean free path λ_{p-air}. This method would in fact be the most direct one to measure the p-air inelastic cross section. Subsequently, the latter can be utilized to derive the p-p cross section using the Glauber theory [4].

Neverthless, no existing cosmic ray experiment is capable to directly detect the X_0 distribution, but (in principle) at relatively low energy. As a consequence, ground based cosmic ray experiments are forced to use indirect methods, such as the measurement of extensive air showers.

Two basic techniques are generally employed:
- for a fixed primary energy and zenith angle, the distribution of the average depth of the shower maximum has an exponential tail, whose slope is releted to the absorption length Λ;
- the absorption length Λ is derived from the distribution of the shower intensity while the zenith angle, i.e. atmospheric depth, increases, for fixed primary energy and shower age.

The last method has been adopted in the ARGO-YBJ experiment. It was initially applied to a data set taken by a limited portion of detector ($\sim 1800\ m^2$ of active area) [5], just as a test of applicability of the technique. Successively, it was used to analyze a reduced set of data collected by the whole central detector ($\sim 5600\ m^2$) [6], with very promising results. In this paper, the analysis of a much larger data set through this method, in order to measure the p-air *production* cross section and to derive the p-p total cross section in the energy range $1 - 100\ TeV$, will be presented and discussed.

II. THE ARGO-YBJ EXPERIMENT

As a result of the collaboration between INFN (Italy) and Chinese Academy of Science, the ARGO-YBJ (*Astrophysical Radiation with Ground-based Observatory at YangBaJing*) experiment [7] exploits the full-coverage technique and the high altitude operation in order to deeply investigate cosmic radiation physics. In more details, through the observation at high altitude of Extensive Air Showers (EASs) produced in the atmosphere by primary photons and nuclei, ARGO-YBJ is able to inspect a wide range of fundamental issues in cosmic ray and astroparticle physics:

- very high energy γ-ray astronomy, with an energy threshold of a few hundreds GeV;
- search for emission of gamma ray bursts in the full $GeV - TeV$ energy range;
- study of cosmic rays (spectrum, composition, $\overline{p}/p$ ratio measurement, shower space-time structure, ...) starting at TeV energies;
- Sun and heliosphere physics above $E_{thresh} \sim 1\ GeV$.

The experiment is running in the Cosmic Ray Laboratory of Yangbajing, 90 km North-West of Lhasa, in the Tibet region (People's Republic of China), at an altitude of 4300 m a.s.l., corresponding to a vertical atmospheric depth of $606\ g/cm^2$.

The apparatus, extensively described in [8], consists of a single layer detector logically divided into 154 units called *clusters* ($7.64 \times 5.72\ m^2$), each made by 12 Resistive Plate

[1]INFN - Sezione di Lecce, via Arnesano, 73100 Lecce, Italy, surdo@le.infn.it

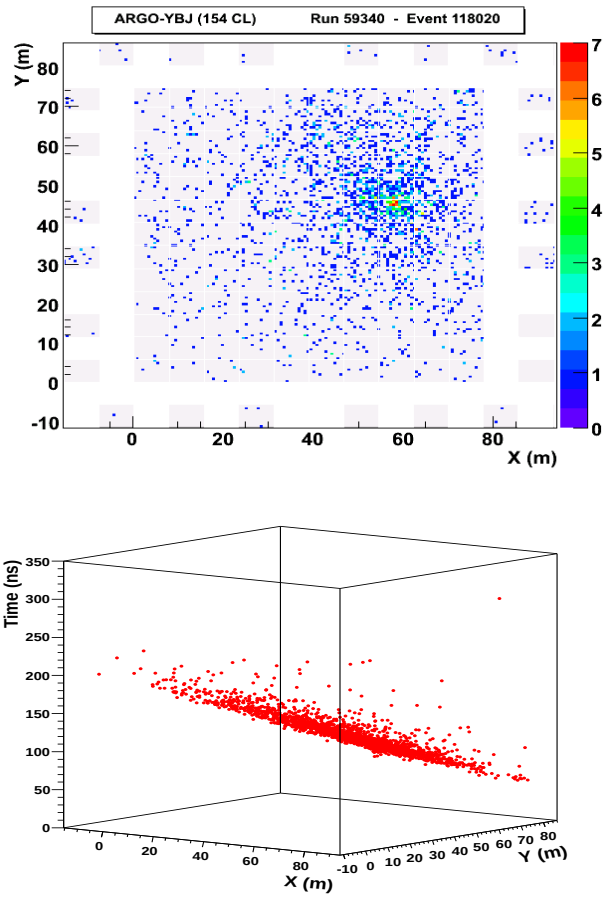

Fig. 1. Two different views of a shower detected by ARGO-YBJ. The hit map at ground is given on top, the color code representing the strip mutiplicity of each fired pad. A space-time view of the shower front is given on the bottom.

Chambers (RPCs) operated in streamer mode. Each RPC ($1.26 \times 2.85\ m^2$) is read out by using 10 pads ($62 \times 56\ cm^2$), which are further divided into 8 strips ($62 \times 7\ cm^2$) providing a larger particle counting dynamic range. The signals coming from the strips of a given pad are sent to the same channel of a multi-hit TDC. The whole system provides a single hit (pad) time resolution at the level of $\sim 1\ ns$, which allows a detailed three-dimensional reconstruction of the shower front with unprecedented space-time resolution (Fig. 1). Moreover, the analog RPC charge readout is going to be implemented.

Nowadays, the 130 clusters of the whole full-coverage central carpet ($\sim 5600\ m^2$) are in smooth data taking since July 2006. In the meantime, the external guard ring has been instrumented and included in the DAQ system since 2007.

III. The Analysis Method

The analysis is based on the shower flux attenuation for different zenith angles, i.e. atmospheric depths, and exploits the detector accuracy in reconstructing the shower properties.

Given a primary energy interval, the frequency of showers as a function of the zenith angle θ, for a fixed distance X_{dm} between the detector and the shower maximum, is directly related to the distribution of the depth of the shower maximum itself, $P(X_{max})$, with $X_{max} = h_0 sec\theta - X_{dm}$, where h_0 is the observation vertical depth. The shape of $P(X_{max})$ is given by the folding of the exponential dependence of the depth of the first interaction point X_0 (i.e. e^{-X_0/λ_p} with $\lambda_p(g/cm^2) \simeq 2.41 \cdot 10^4/\sigma_{p-air}(mb)$), with the probability distribution of $X_{rise} = X_{max} - X_0$, which takes into account the fluctuations of the shower development up to its maximum. For sufficiently large X_{max} values, $P(X_{max})$ tends to have a simple exponential falling behaviour with an *absorption length* $\Lambda = k \cdot \lambda_p$, where k depends on the shower development in the atmoshpere, on its fluctuations and on the detector response. The actual value of k must be evaluated by Monte Carlo (MC) simulations, and it might in principle depend on the features of the adopted hadronic interaction model, even if several studies showed that the dependence is small. Finally, the contribution of cosmic rays heavier than protons have to be estimated, or at least minimized in the analyzed data sample, in order to get an unbiased p-air cross section estimate.

For EAS detectors like ARGO-YBJ, which measures the particles at ground, the $P(X_{max})$ distribution might be sampled through the flux dependence on the zenith angle, once X_{dm} (or the shower age) has been fixed or constrained, within the limits of detector capabilities. Really, it is simply to show that the exponential tail of that distribution can be accessed by selecting the showers with the maximum development not far from the detection level (i.e. by mimizing X_{dm}) and, obviously, exploring a zenith angle region as wide as possible.

The ARGO-YBJ detector location (that is small atmospheric depth) and features (full-coverage, angular resolution, fine granularity, etc.), which ensure the capability of reconstructing the detected showers in a very detailed way, have been used to fix the energy ranges and to constrain the shower ages. In particular, different hit (i.e. strip) multiplicity intervals have been used to select showers corresponding to different primary energies, while the information on particle density, lateral profile and shower front extension have been used to constrain X_{dm} in a range that makes possible the observation of the exponential falling of shower intensities, through the $sec\theta$ distribution. In the real data set, the fit to this angular distribution with an exponential law gives the slope value α, connected to the (observed experimental) absorption length Λ^{exp} through the relation $\Lambda^{exp} = x_0/\alpha$, that is:

$$I(\theta) = A(\theta) I(\theta = 0) \cdot exp(-\alpha \cdot (sec\theta - 1)) \qquad (1)$$

where $A(\theta)$ accounts for the geometrical acceptance of each angular bin and $x_0 = 606\ g/cm^2$ (vertical atmospheric depth).

The same procedure is applied to the simulated sample (see next section for the details about the Monte Carlo simulation). For each strip multiplicity interval, the fit of the $sec\theta$ distribution with the exponential function of Eq. 1 allows to obtain the value of the (observed simulated) absorption length Λ^{MC}.

The value of k, which refers to each strip mutiplicity bin, can then be evaluated as $k = \Lambda^{MC}/\lambda_{int}^{MC}$. The interaction length λ_{int}^{MC} is given by the average value of the MC proton interaction length distribution, corresponding to the selected events in the considered multiplicity bin.

The experimental interaction length is obtained by correcting the observed absorption length, Λ^{exp}, by the factor k previously determined on the basis of the MC simulation: $\lambda_{int}^{exp} = \Lambda^{exp}/k$. Such value will give the measured p-air interaction length (λ_{p-air}^{exp}), once the effects of heavier nuclei contained in the primary cosmic ray flux have been accounted for. In the present analysis, this has been made by evaluating the contribution to the slope α (see Eq. 1) produced by the addition of a proper Helium fraction to the proton primary flux in the MC simulation, the contribution of nuclei heavier than Helium being negligeable.

The p-air *production* cross section is obtained from the aformentioned relation: σ_{p-air} (mb)$= 2.41 \cdot 10^4/\lambda_{p-air}^{exp}$ (g/cm^2), while several theoretical models can be used to get the corresponding p-p total cross section σ_{p-p} (see Sec. V).

IV. Data Selection and Monte Carlo simulation

The above described analysis was applied to a data sample of about 6.5×10^8 events collected by the 130 clusters of the central detector with a 20 pad threshold inclusive trigger. In order to have both a small contamination of external events (i.e. those events with the true core position outside the carpet but reconstructed inside) and an angular resolution better than 0.5°, only events with $\geq$ 400 fired strips were considered. Moreover, the analysis was restricted to those events with reconstructed zenith angle in the range $0° < \theta_{rec} < 40°$, in order to avoid the effects due to the possible zenith angle dependence of the analysis cuts.

After a first selection based on the quality of the reconstruction procedure, a further rejection of external core showers was performed by means of several additional cuts discussed in the following. The reconstructed core position, P_{rc}, was required to be in a fiducial area given by the inner 8×11 RPC clusters (corresponding to a total surface of about $64 \times 64\ m^2$). This cut reduced the initial data set (with $\theta_{rec} < 40°$ and $N_{strip} \geq 400$) to about 45%. The quantity R_{70} was then defined as the radius of a circle (centered in P_{rc}) containing 70% of the fired strips and it was required that the distance of P_{rc} from the detector center plus R_{70} was less than $50\ m$. The aim of this cut was to select that showers largely contained inside the detector area, thus well reconstructed. As a result of this condition, the data sample was reduced to $\sim 20\%$ with respect to the initial one. One further cut required the minimum average fired strip density, within a distance R_{70} from the reconstructed core, to be $\sim 0.2/m^2$ (in the shower plane). Such "density cut" allowed to furtherly reject some misreconstructed internal core events, as shown in Fig. 2. The same purpose motivated the last selection cut (a "compactness cut"), requiring the R_{70} radius to be at most $30\ m$. The MC simulation (see below) showed that this "compactness cut" is also related to the shower development stage, thus allowing to constrain the value of X_{dm} (Fig. 2). Those last two cuts finally selected $\sim 10\%$ of the events reconstructed with $\theta_{rec} < 40°$ and $N_{strip} \geq 400$, which constitute the initial data set.

The surviving data sample was finally split into six different bins of fired strips ΔN_{strip} (see tables in the following),

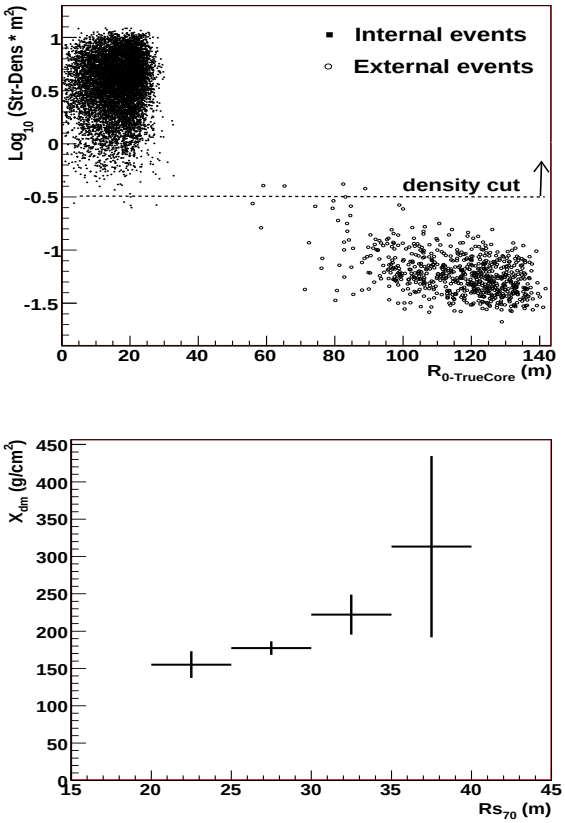

Fig. 2. Top. Strip density near the reconstructed core vs distance of the true core from the detector center, for a sample of E = 30 TeV p initiated showers: the "density cut" described in the text (i.e. $Log(Str{-}Dens{*}m^2) > -0.5$) is able to reject most misreconstructed core events (labeled as 'External events'). Bottom. Correlation between R_{70} (see the text) and X_{dm}: the cut at $R_{70} < 30$ allows to select low X_{dm} (i.e. deeper maximum) events.

each one corresponding to a different primary energy interval, starting from the threshold of at least 400 strips fired on the whole central detector (out of the $124,800$ contained into 130 clusters), in the trigger time window of $\sim 400\ ns$.

A suitable simulation chain was used in order to tune the values of the different analysis cuts, check their effects and have an estimation of the possible systematics. About 10^8 proton initiated and 2×10^7 He initiated showers, with the proper power law energy spectra between $300\ GeV$ and $3000\ TeV$ and zenith angle up to 45°, were produced with the *CORSIKA* code [9], using *QGSJET* as hadronic interaction model [10]. A full simulation of the detector response, based on the GEANT3 package [11] and also including the effects of time resolution, trigger logic, electronics noise, etc., was performed. Monte Carlo data have been analyzed by using the same reconstruction code as for real data.

The reliability of the simulation procedure was successfully checked in several ways, concerning in particular the observables mostly involved in selection cuts and primary energy determination. The comparison between various quantities (used in the analysis) from the real and the simulated data sample showed a more than satisfactory agreement both before

TABLE I

THE STRIP MULTIPLICY INTERVALS, THE CORRESPONDING PRIMARY ENERGIES, THE RELATED AVERAGE INTERACTION LENGTH AND THE CORRESPONDING CORRECTION FACTORS k (SEE TEXT).

ΔN_{strip}	$\langle E_p \rangle (TeV)$	$\lambda_{int}^{MC} (g/cm^2)$	k
$400 \div 1000$	4.0	78.5 ± 2.1	$2.01 \pm 0.06 \pm 0.05$
$1000 \div 2000$	8.3	76.2 ± 1.8	$1.53 \pm 0.02 \pm 0.04$
$3000 \div 4000$	19.8	73.4 ± 1.5	$1.59 \pm 0.04 \pm 0.03$
$6000 \div 8000$	38.7	71.4 ± 1.3	$1.68 \pm 0.06 \pm 0.03$
$8000 \div 12000$	53.5	70.5 ± 1.2	$1.71 \pm 0.07 \pm 0.03$
> 8000	76.7	69.5 ± 1.6	$2.05 \pm 0.06 \pm 0.05$

and after the adopted event selection cuts.

Moreover, the fractions of events surviving the analysis cuts were checked to be consistent with the corresponding quantities for the real data sample. All numbers were in nice agreement. For instance, $\sim 11\%$ of the starting sample of MC events actually came through all the analysis cuts, consistent with the aforementioned value found for the real data ($\sim 10\%$).

As already stated, each strip multiplicity interval corresponds to a different primary energy range, as shown in Tab. I, where the value $\langle E_p \rangle$, obtained from the average of the MC logarithmic energy distribution, is reported. Using the simulation, it has been verified that the energy scale assigned in this way ($\langle E_p \rangle$) is equivalent to that given by the median energy of the corresponding events, E_{50}, or by the value, E_λ, corresponding to the average λ_{p-air}^{MC} in the selected sample.

As an example, Fig. 3 shows the logarithmic primary energy distribution and the related p-air interaction length distribution for the strip multiplicity interval $\Delta N_{strip} = (1000 \div 2000)$.

Simulations have also shown that, after all analysis cuts were applied, the contamination of external events misreconstructed as internal ones is $\epsilon \simeq 10\%$ in the first multiplicity interval ($N_{strip} = 400 \div 1000$), while it is less than 1% for all the higher energy bins ($N_{strip} > 1000$).

Finally, a check has been made that the event selection, both in primary energy and shower age (or X_{dm}), was independent on the zenith angle up to about 40° (as shown in Fig. 4), thus verifying that our experimental sensitivity is not compromised by the shower fluctuations [13], [14].

V. ANALYSIS RESULTS AND DISCUSSION

The result of applying the whole selection procedure to the real data is given in Fig. 5, where the experimental $sec\theta$ distributions for the six strip multiplicity (i.e. energy) intervals are shown, after having corrected for the geometrical acceptance of each angular bin. They clearly show the expected exponential behaviour, this being a further check that the detector capabilities and the adopted analysis cuts allowed a proper selection of events for the cross setion measurement. A slight deviation is present, for the lowest energy sample only, at small $sec\theta$ values (therefore not included in the fit). This is accounted for the larger contamination of external events in this strip multiplicity bin (see Tab. I), even if there might also be a contribution of shower fluctuations, the shower maximum being more distant from the detector for these events

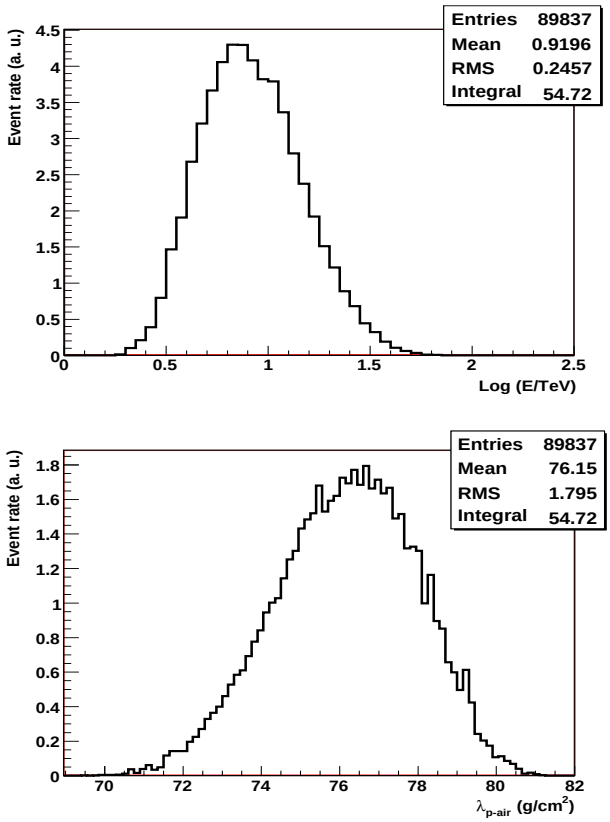

Fig. 3. Logarithmic primary energy distribution (top plot) and interaction length distribution (bottom plot) for the MC proton initiated shower sample with strip multiplicity interval $1000 < N_{strip} < 2000$.

(for the lowest energy sample $\langle X_{max} \rangle \simeq 390\,\mathrm{g/cm^2}$, while $\langle X_{max} \rangle \simeq 450\,\mathrm{g/cm^2}$ for the other ones).

The angular distributions obtained in the same way from the MC simulation show very similar behaviours to that of the real data and the same considerations can be applied. From these plots, the values of Λ^{MC} are extracted by fitting them to an exponential function, with slope parameter given by $\alpha = h_0^{MC}/\Lambda^{MC}$, where $h_0^{MC} = 606.7\ g/cm^2$ (the nominal atmospheric depth corresponding to the altitude of $4300\ m\ a.s.l.$). Such values, once divided by the corresponding average λ_{int}^{MC} of Tab. I, give the values of the parameter k for the different energies. The results are reported in the same table, where both the statistical and the systematic errors are also shown. The first one comes from the fit procedure, while the second one has been calculated on the basis of the root mean square (rms) values of the λ_{int}^{MC} distributions.

As it can be seen, the k values are all in the range $1.5 \div 1.7$, apart those obtained for the lowest and the highest primary energy intervals. The relatively high value of k for the lowest energy bin has been ascribed to the larger contamination of the external events. This hypothesis has been verified by estimating k from the truly internal events only, thus obtaining a value $k \simeq 1.6$, in agreement with that found at larger energies. As far as the highest energy interval is concerned, the reason for the relatively high value of k is not so obvious,

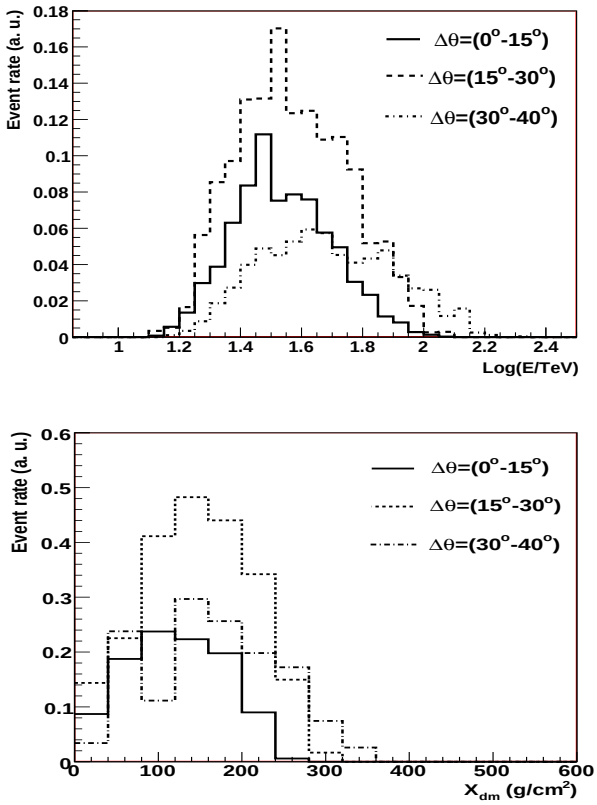

Fig. 4. Top: logarithmic primary energy distribution after all selection cuts for the three zenith angle intervals: $0-15^\circ$, $15-30^\circ$ and $30-40^\circ$. Bottom: distribution of X_{dm} (slant distance between shower maximum depth and detection level) for the same angular bins.

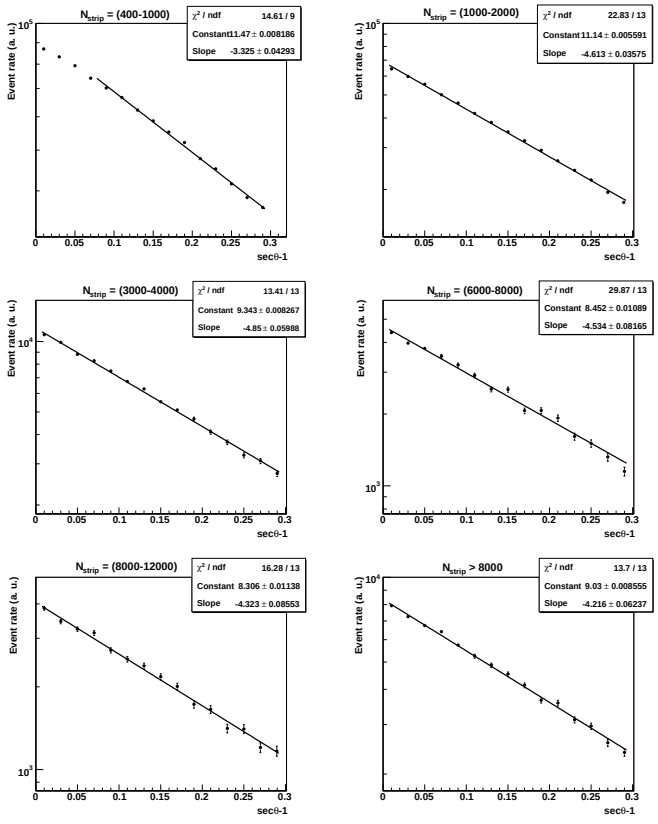

Fig. 5. Experimental $sec\theta$ distributions for the six strip multiplicity samples, after the selection cuts and the correction for the geometrical acceptance in each angular bin.

a possible explanation being the beginning of saturation of the strip digital information used in the analysis. This makes wider the energy interval contributing to the related multiplicity bin (as the larger ϵ does at the lowest energies), therefore implying a larger effect of the shower to shower fluctuations, mainly in terms of X_{rise}, with a consequent loss of sensitivity. Those two effects practically define the energy region where the current analysis can be applied. Important improvements could be achieved by using more detailed information on the lateral profile and the shower front (curvature, rise time, time width, etc.), that ARGO-YBJ is able to record with high precision, and especially with the use of the analog RPC readout.

One source of uncertainty in the p-air cross section measurement is given by the variations of h_0 (see Eq.1) due to the changing atmospheric pressure with time. From the pressure data continuously taken at YangBaJing, we evaluated $h_0^{MC}/h_0 = (0.988 \pm 0.007)$, resulting in an impact on the cross section analysis at level of 1%. The cross section data presented here have been already corrected for this effect.

As outlined in Sec. III, the measured absorption length (Λ^{exp}) values, together with the correction of the k factors determined from the simulation, directly give the experimental interaction length (λ_{int}^{exp}) and consequently the production cross section σ_{int}. This has still to be corrected for the contribution of heavier primaries.

The correction due to the presence of cosmic ray primaries heavier than protons has been estimated by evaluating the effect on the shape of the $sec\theta$ distribution by the introduction of Helium primaries in the simulated data. Both the different absolute values and the energy dependences of proton and Helium fluxes were considered, by taking as a reference the fits to the experimental data given in [12]. As expected, the simulations showed a slight steepening of the $sec\theta$ distribution at the highest strip multiplicity intervals (that is energies), thus changing the values of the corresponding cross section estimates. By adopting this procedure we got the correction factors η to be applied to σ_{int}. These are reported in Tab. II, for the six primary energy values. The effect of the uncertainty of the primary cosmic ray composition has been evaluated by applying the above procedure starting from two different primary flux measurements given in the literature, namely those from the JACEE and RUNJOB experiments. We found small differences (at most within 4%), which were used as an estimation of the systematic error on the correction η, as reported in Tab. II.

The resulting p-air production cross sections, σ_{p-air}, for the considered six primary energy values, are summarized in Table II, where both statistical and systematic errors (propagated separatly through all the analysis flow) are indicated. These

TABLE II

THE STRIP MULTIPLICY INTERVALS, THE CORRESPONDING PRIMARY ENERGIES, THE RELATED CORRECTION FACTORS FOR THE HELIUM CONTRIBUTION, η, AND THE P-AIR CROSS SECTIONS THUS OBTAINED. BOTH STATISTICAL AND SYSTEMATIC ERRORS ARE REPORTED.

ΔN_{strip}	$\langle E_p \rangle (TeV)$	η	σ_{p-air} (mb)
$400 \div 1000$	4.0	$1.00 \pm 0.04 \pm 0.01$	$261 \pm 13 \pm 8$
$1000 \div 2000$	8.3	$1.00 \pm 0.02 \pm 0.01$	$278 \pm 7 \pm 7$
$3000 \div 4000$	19.8	$1.00 \pm 0.04 \pm 0.01$	$303 \pm 15 \pm 7$
$6000 \div 8000$	38.7	$0.96 \pm 0.05 \pm 0.03$	$288 \pm 19 \pm 11$
$8000 \div 12000$	53.5	$1.00 \pm 0.05 \pm 0.03$	$289 \pm 19 \pm 10$
> 8000	76.7	$0.95 \pm 0.04 \pm 0.04$	$322 \pm 17 \pm 16$

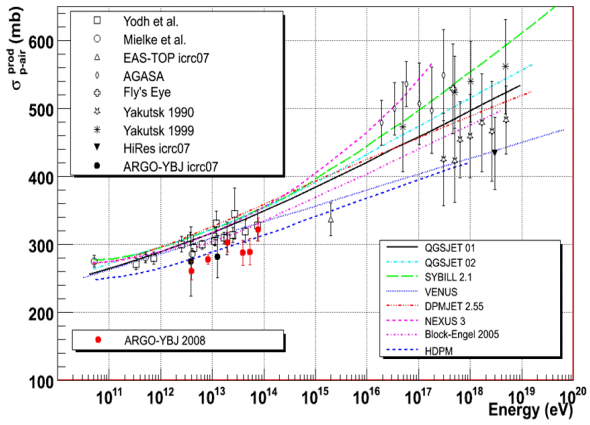

Fig. 6. The proton-air *production* cross section as measured by ARGO-YBJ and by different cosmic ray experiments. The prediction of several hadronic interaction models are also shown. Only the statistical errors are drawn.

results are consistent with those of previous already mentioned ARGO-YBJ works ([5], [6]) not using the strip information.

The measured p-air production cross section is shown in Fig. 6 as a function of the primary proton energy. As it can be seen, the results reported in this paper are in agreement with other measurements. In particular, the relatively low energy threshold of ARGO-YBJ makes possible a direct comparison with the data of single hadron flux at ground. The predictions of several hadronic interaction models are also shown. Our results look to prefer models which predict smaller p-air production cross section values in the considered energy range.

It was outlined in Sec. I that the p-p total cross section σ_{p-p} can be inferred from the measured p-air production cross section σ_{p-air} by using the Glauber theory [4], as discussed in several papers. We applied the conversion reported in [15] and took the differences among different models, that in our energy range are approximately within 5%, as a separate further contribution to the systematic error on σ_{p-p}. The preliminary results, for the six energy bins, are summarized in Fig. 7. It can be seen that the ARGO-YBJ data lie in an energy region until now unexplored by accelerator experiments and permit of better investigating the behaviour of the p-p total cross section where it starts to significantly increase with energy.

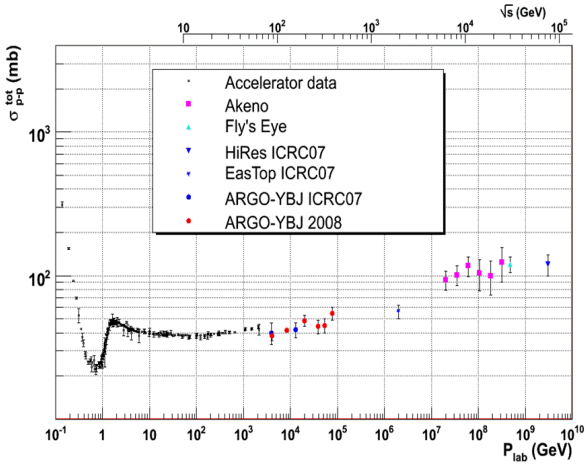

Fig. 7. Preliminary p-p total cross section obtained by ARGO-YBJ starting from σ^{prod}_{p-air}, together with that found by other cosmic ray experiments. The accelerator data are also reported. Only the statistical errors are drawn.

VI. CONCLUSION

The analysis of the ARGO-YBJ data collected with the $\sim$ 5600 m^2 of the central full-coverage detector allowed us to measure the proton-air production cross section and, consequently, to obtain a first estimate of the proton-proton total cross section in an energy region until now unexplored by accelerator experiments. The results are in agreement with previous (preliminary) ARGO-YBJ results and allow to inspect the behaviour of the p-p cross section where it starts to increase, as drawn by the data of $p\overline{p}$ colliders and of extremely high energy cosmic ray experiments. Thus, it appears again important the extension of the analysis to $\sim PeV$ energies, by using the information from the analog RPC readout.

REFERENCES

[1] N.A. Amos et al., *Phys. Rev. Lett.* (1992) 2433
[2] F. Abe et al., *Phys. Rev.* **D50** (1994) 5550
[3] C. Avila et al., *Phys. Lett.* **B445** (1999) 419
[4] R.J. Glauber and G. Matthiae, *Nucl. Phys. B*, vol.21, p.135, 1970; L. Durand and H. Pi, *Phys. Rev D*, vol.38, p.78, 1988; T. Wibig and D. Sobczynska, *J. Phys. G: Nucl. Part. Phys.*, vol.24, p.2037, 1998.
[5] A. Surdo et al. (ARGO-YBJ Collab.), *Proc. of the 20th European Cosmic Ray Symposium*, Lisbon, Portugal (2006)
[6] I. De Mitri et al. (ARGO-YBJ Collab.), *Proc. of 30th International cosmic Ray Conference*, Merida, Mexico, Session HE.3.1, No.950 (2007)
[7] M. Abbrescia et al. (ARGO-YBJ Coll.), *Astroparticle Physics with ARGO*, Proposal (available at http://argo.na.infn.it), 1996.
[8] G. Aielli et al. (ARGO-YBJ Coll.), *Nucl. Inst. and Meth. in Phys. Res. A*, vol.562, p.92, 2006.
[9] J. Knapp and D. Heck, *Extensive Air Shower Simulation with CORSIKA (6.203)*, 1998.
[10] N. N. Kalmykov et al., Nucl. Phys. B, Proc. Suppl. **52**, (1997) S. Ostapchenko, Nucl. Phys. B, Proc. Suppl. **151**, 143 (2006)
[11] GEANT - Detector Description and Simulation Tool, CERN Program Library, Long Writeup, W5013 (1993)
[12] J.R. Hörandel, Astropart. Phys., **19** (2003) 193
[13] J. Alvarez-Muniz et al., *Phys. Rev.* **D66** (2002) 123004
[14] J. Alvarez-Muniz et al., *Phys. Rev.* **D69** (2004) 103003
[15] M.M. Block, Phys. Rev. **D76** (2007) 111503